SSRG International Journal of Electrical and Electronics Engineering
ISSN: 2348-8379/ https://doi.org/10.14445/23488379/IJEEE-V13I5P105

Volume 13 Issue 5, 48-61, May 2026

Original Article

Comparative Evaluation between Monofacial and Bifacial Modules under a Probabilistic Reliability Approach

Oscar Saul Umasi Mendigure[1], Wilson Jose Mamani Huanca[2], German Alberto Echaiz Espinoza[3], Wilson Omar Ramos Parqui[4]

[1,2,3,4]*Universidad Nacional de San Agustin de Arequipa, Arequipa, Perú.*

[1]*Corresponding Author : oumasi@unsa.edu.pe*

Received: 10 February 2026 Revised: 09 March 2026 Accepted: 08 April 2026 Published: 30 May 2026

Abstract - *This study compares monofacial and bifacial photovoltaic modules in a 100 MWp power plant located in Tacna, Peru, using a probabilistic reliability approach. The methodology is based on Markov chains to represent the failure and repair behavior of system components, from the PV modules to the transformer, together with the construction of COPT tables to calculate the energy indices ISE, ESE, and Ae. For the analysis, hourly irradiance data over one year were considered, and in the case of bifacial modules, a variable gain throughout the day was adopted to capture the effect of reflected radiation. The results indicate that bifacial modules lead to higher energy indices compared to monofacial modules, with ISE increasing from 44,641,058.05 to 50,575,054.85 and ESE from 44,023,905.25 to 49,875,865.86, representing an increase of about 13.3%. However, when energy availability is evaluated, the monofacial system shows a higher value (Ae = 0.9858) compared to the bifacial system (Ae = 0.9321), indicating that a higher energy gain does not necessarily translate into higher final availability. In this sense, combining reliability modeling with energy performance analysis provides a more realistic assessment of the performance of large-scale photovoltaic power plants.*

Keywords - *Bifacial Photovoltaics, Copt, Diffuse Fraction, Monofacial Photovoltaics, Reliability.*

1. Introduction

The growth of photovoltaic generation has become one of the main pillars of the global energy transition, mainly due to its contribution to reducing Greenhouse Gas (GHG) emissions. In recent years, technological advances combined with cost reductions have driven a rapid market expansion, supported by improvements in cell architecture and in the materials used for both modules and inverters [1]. As a result, the installed photovoltaic capacity increased from 1,645 GWp in 2023 to 2,247 GWp in 2024, representing an addition of 602 GWp in a single year and confirming the accelerated global deployment of this technology [2].

This expansion has also been accompanied by continuous technological evolution, reflected in improved energy performance, better operational reliability, and enhanced integration with the electrical grid. In this context, bifacial photovoltaic modules have gained attention, since they are capable of generating energy from both the front and rear surfaces, unlike conventional monofacial modules that only use front-side irradiance. Moreover, when combined with solar tracking systems, bifacial modules can further increase energy production and contribute to reducing the Levelized Cost Of Energy (LCOE). However, bifacial gain is not constant and depends on several installation and environmental factors, such as ground conditions, module height, and tilt angle [3]. For this reason, bifacial systems have been increasingly adopted in medium- and large-scale photovoltaic plants, not only due to their higher energy yield, but also because they represent a trend toward better utilization of the available solar resource [4].

From an operational perspective, there is an increasing demand for higher energy efficiency, improved reliability, and cost optimization. Nevertheless, the availability of photovoltaic systems is still strongly influenced by the behavior of critical components, especially inverters, whose failure can significantly reduce power generation. In addition, degradation mechanisms and local environmental conditions can modify failure rates and failure modes, directly affecting system availability and energy delivery [5]. Both monofacial and bifacial systems are subject to losses caused by resource variability and component failures. However, in bifacial systems, these effects can be more complex, since both front and rear irradiance contributions may be affected depending on the surrounding conditions and ground characteristics [6].

Another important aspect is related to soiling and energy yield optimization. In desert environments, differences in performance have been observed depending on module configuration and maintenance strategies. For example, a study conducted in Qatar showed that tilted bifacial modules produced, on average, 4.0% more annual energy than vertical configurations under clean conditions. On the other hand, vertical configurations presented lower dust accumulation, reducing cleaning requirements [7].

Despite these advances, there is still a gap in the evaluation of energy performance under real operating conditions. This is mainly because bifacial gain varies with installation parameters such as module spacing, height, tilt, and orientation, as well as environmental factors like ground albedo and soiling conditions [7-9]. Addressing this gap is important for improving plant design and operation, since a combined analysis of energy performance and reliability can reduce uncertainties associated with energy losses and support better decision-making.

Despite these advances, most studies still focus on energy performance analysis, bifacial gain estimation, and validations under specific conditions, with limited attention to the integration of energy performance and probabilistic reliability modeling at the utility scale. In addition, the impact of component failures and repair processes on the actual energy delivered by bifacial systems is still little explored, and comparative analyses between bifacial and monofacial systems considering the effectively delivered energy are not frequently addressed. This makes it difficult to understand whether the higher generation potential of bifacial systems actually translates into better overall performance when reliability aspects are considered. For this reason, a more comprehensive approach is needed, combining energy production analysis with system reliability. In this context, this work proposes a comparative approach between monofacial and bifacial photovoltaic systems based on probabilistic reliability modeling, integrating Markov chains, failure and repair rates, and COPT-based energy indices, allowing a joint evaluation of energy generation and system availability and providing a more complete assessment under real operating conditions, especially for large-scale photovoltaic power plants.

1.1. Literature Review

Reference [10] presents a systematic review of bifacial photovoltaic module technologies. The focus of this study is on the characteristics of bifacial modules, as well as modeling, performance, applications, and future trends and challenges. For this purpose, studies published between 2010 and 2022 were compiled. The results show that bifacial photovoltaic modules can generate up to 30% more energy under optimal conditions, but in real photovoltaic power plants, the gain is usually between 5% and 25%. The study also includes a technical and economic comparison with monofacial modules, including performance metrics and LCOE analysis. Even though different modeling and performance methodologies are reviewed, the study does not propose a specific method. In addition, it does not address system reliability or availability, nor does it consider an analysis based on component failure and repair rates.

A comparative experimental study between bifacial and monofacial photovoltaic systems is carried out in [11] using a solar plant located in the United Kingdom. The study evaluates the I–V and P–V curves under the same environmental conditions and also analyzes the influence of installation parameters such as installation height, tilt angle, environmental conditions, and ground albedo. The performance of both systems is evaluated under different operating conditions. The methodology is based on real plant data, where irradiance and energy production data are analyzed. The results indicate that the bifacial gain strongly depends on the ground albedo, varying between 6% and 15% for green surfaces and between 17% and 56% for white substrates. In addition, bifacial modules reached efficiencies close to 18%, while monofacial modules ranged between 11% and 13%. Although the study is quite complete, it does not consider parameters related to component failure rates, and it also does not include a temporal modeling approach that would allow a more complete evaluation of plant behavior, since no reliability analysis is performed.

A comparison between bifacial and monofacial modules to analyze the efficiency and energy generation of these technologies is presented in [12]. The main focus of the study was to evaluate the influence of tilt angle, installation height, and ground albedo on module performance. For this purpose, data under real environmental conditions were analyzed using a 390 W LG NeON bifacial module and, to represent the monofacial module, the rear side was covered with a film to prevent irradiance capture. The tests were conducted in Poland between July and August 2022, considering different tilt angles, different mounting heights, and different ground albedo conditions. The results showed that bifacial modules had better performance than monofacial ones, and that this gain depends strongly on the installation characteristics. Under more favorable conditions, the instantaneous power increase exceeded 56%, and in the annual estimate, the gain reached up to 14.3% compared to the monofacial module. One of the most notable results was observed under high-albedo conditions, with a white substrate and a height of 1 m above the ground. Even so, the study focuses more on the energy performance aspect and does not further address the reliability of the system as a whole, nor does it present a probabilistic analysis of the behavior of the components over time.

The reliability and performance of photovoltaic inverters operating with bifacial and monofacial modules are analyzed in [13]. The study evaluates inverter operation under higher loading conditions due to the use of bifacial modules, since

the inverter operates for a longer time, and the thermal stress can reduce its lifetime. In the methodology, a 3 kW grid-connected system was considered, with an annual analysis carried out in Hyderabad, India. The work integrates the electrothermal modeling of the IGBT junction temperature using the Foster model and, for the reliability analysis, a Monte Carlo simulation with 10,000 samples and a 5% variation, fitted to a Weibull distribution, was performed. The analysis was conducted at both the component and system levels. For the scenarios, three cases were considered with 0%, 30%, and 50% more energy generation compared to monofacial modules. In the case of monofacial modules, the reliability was higher, with a B10 lifetime of 34 years at the component level and 24 years at the system level. In the case of bifacial modules, a progressive reduction was observed, decreasing from 34 years in the reference case to 5 years in the scenario with 30% more energy, and to 1.5 years in the scenario with 50% more energy. Although this work represents an important step toward a reliability-oriented assessment, it is limited to inverter analysis and does not evaluate energy reliability indices of the power plant as a whole.

A performance comparison between monofacial and bifacial photovoltaic modules under temperate climate conditions is carried out in [14], with a focus on industrial rooftop applications. The objective is to understand how the modules behave under real operating conditions, considering factors such as irradiance, temperature, diffuse fraction, and mounting structure.

The analysis was conducted in Milan, Italy, where three modules were compared, including two monofacial modules and one bifacial module. The I–V curves were evaluated under different atmospheric conditions. The results showed a higher gain for the bifacial module compared to the two monofacial modules, reaching 4.3%, 5.4%, and 6.4% in relation to the first one, and 5.0%, 6.4%, and 7.8% in relation to the second module. However, the study focuses on performance evaluation and does not include reliability analysis or system availability assessment.

A probabilistic evaluation of the reliability of a 1 MWp photovoltaic power plant with string topology is presented in taking Arequipa, Peru, as a case study. The objective of the analysis was to individually estimate the failure and repair rates of each component of the system while also considering the variability of solar irradiance. The authors used an approach based on Markov chains and the probability mass function of irradiance. The main results obtained were ISE = 2,277.02 MWh, ESE = 2,179.95 MWh, and an availability of 0.9573, showing good system availability. However, the study did not evaluate a comparative analysis between monofacial and bifacial modules. In addition, the analysis was carried out for a specific location, which may limit the generalization of the results to other climatic and geographical conditions. Operational data from a 34.7 MW photovoltaic power plant in North Yorkshire, United Kingdom, are evaluated in [11], considering operation data from 2020 to 2024. The authors analyze the real energy performance of monofacial and bifacial modules over several years of operation, in addition to evaluating degradation behavior and the influence of environmental factors such as ground albedo, irradiance, and snow.

The results showed gains between 15.12% and 17.31% in comparison with traditional modules, although the bifacial modules also exhibited slightly higher annual degradation rates. In this study, 91,392 bifacial modules were evaluated, and the NREL RdTools tool was used for the analysis. The work presents a comparison between the modules and their energy efficiency and shows that, despite the influence of environmental factors, higher gains were observed in the bifacial modules compared to the monofacial ones, even under different climatic conditions. However, no reliability or system availability analysis was carried out. A reliability and criticality analysis of a large-scale photovoltaic system is presented in [15] using the Fault Tree Analysis approach. The authors used a methodology to model the reliability of a grid-connected system, with a focus on the components and failures on the DC side of the system. The work aims to identify which failures are the most critical for reducing system performance and reliability. For this purpose, failure and repair rate data obtained from the literature were used. The results showed that the highest criticality factors were found in the cases of fuses, circuit breakers, and PV modules. In the analysis, no comparison of system reliability was made between different types of modules, and no system availability analysis was carried out.

The performance of monofacial and bifacial Silicon Heterojunction (SHJ) photovoltaic modules is evaluated in [16] under desert conditions in Qatar, with a focus on temperature, reflected irradiance, and soiling. The study combines input and output measurements to compare the two technologies and verify which one shows better behavior under this type of climate.

The analyzed period was between 2017 and 2019. The results showed that the bifacial modules achieved 15% higher energy production compared to the monofacial modules. In addition, under clear-sky conditions, the maximum power was about 12% higher than that of the monofacial modules. Regarding soiling, it was observed that bifacial modules are less sensitive to dust accumulation and, therefore, the cleaning frequency can be reduced for this type of module. In this work, the performance of bifacial and monofacial photovoltaic modules was addressed by analyzing energy performance, but not system reliability or availability.

From the literature, it can be observed that different studies have been developed around bifacial photovoltaic

systems, mainly focusing on energy performance, bifacial gain, and analyses under different environmental and installation conditions, while other works evaluate degradation and long-term behavior. There are also studies that address reliability, but they are generally limited to specific components, such as inverters, or do not consider the variability of the solar resource.

In addition, even when probabilistic approaches are applied, they are usually used separately from energy performance analysis, and comparative studies between monofacial and bifacial systems are typically restricted to efficiency or energy generation, without including reliability-based indicators.

As a result, performance and reliability are still treated separately, without an integrated approach at the system level. In this sense, the present work proposes a methodology that allows the joint evaluation of these aspects, providing a more complete assessment of photovoltaic system performance.

2. Analysis Methodology

The methodology follows a direct sequence, as illustrated in Figure 1.

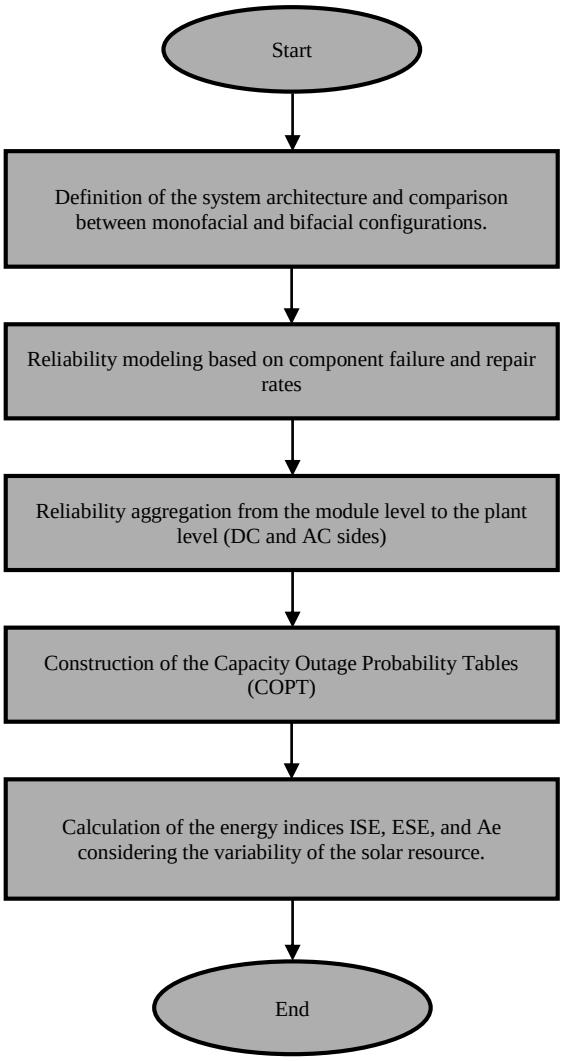

Fig. 1 Overview of the proposed procedure

2.1. System Architecture and Topology

Photovoltaic systems can be implemented using different architectures, among which centralized, string, multi-string, and AC module topologies stand out. Each of these architectures presents different connection structures, control strategies, and levels of operational complexity.

According to [17], string and multi-string architectures offer advantages in terms of mismatch loss reduction and higher reliability, since they allow independent Maximum Power Point Tracking (MPPT) control for groups of modules.

In contrast, centralized systems present a lower cost per installed power unit and a simpler structure. On the other hand, they tend to be more sensitive to partial shading and failures, since the loss of one or more modules can directly affect the overall system performance.

Additionally, [18] shows that the choice of system architecture significantly influences the amount of energy effectively injected into the electrical grid, highlighting the importance of properly selecting the system topology

2.2. Monofacial vs Bifacial Modules

Monofacial photovoltaic modules convert solar energy from the irradiance incident on the front surface and are widely used in conventional systems. In contrast, bifacial photovoltaic modules can capture radiation from both the front and rear surfaces, taking advantage of the light reflected from the ground, as shown in Figures 2 and 3.

In [19], the performance of bifacial and monofacial systems is compared under different ground albedo conditions. The results indicated that, on natural soil, bifacial gain ranged between 5% and 10%, while surfaces with higher reflectance provided increases in energy generation exceeding 20%.

Furthermore, [20] highlights that bifacial technology is becoming established as a new standard in the photovoltaic sector due to its potential to increase energy production. The configuration of bifacial systems may follow different strategies, such as unconstrained operation, in which each layer operates independently; Current-Matched (CM), where the layers share the same current; and Voltage-Matched (VM), in which the voltage is maintained equal between layers. In solar energy harvesting, to maximize it, climatic and environmental factors are considered, such as the type of soil, temperature, module installation, and row spacing, as discussed in [21].

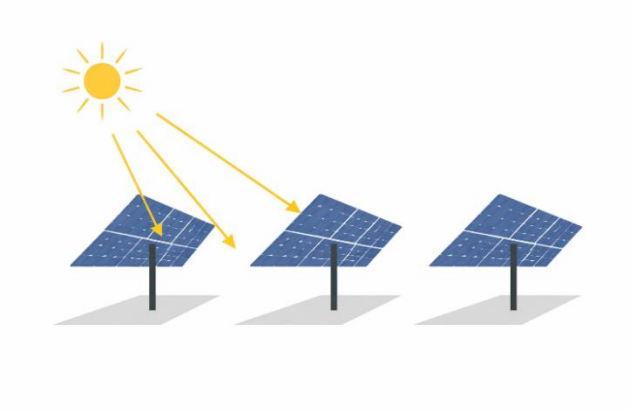

Fig. 2 Irradiance incidence and energy generation in a monofacial module

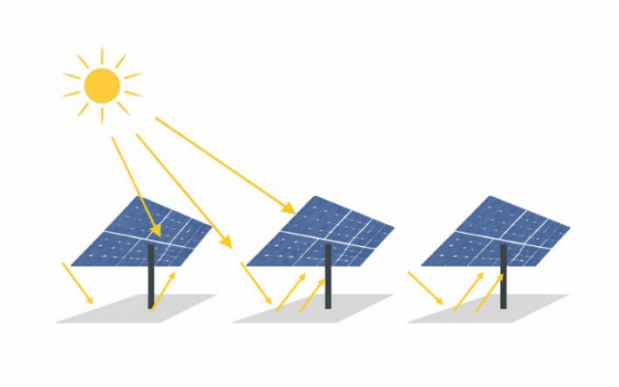

Fig. 3 Front and rear irradiance contribution in a bifacial module

2.3. Reliability Modeling Basis

In this analysis, reliability is defined as the probability that a system performs its intended function under specified conditions for a given period of time. According to [22], this characteristic depends on the operating environment, operational regime, maintenance strategies, and system service time.

In photovoltaic systems, reliability is directly associated with component failure and repair rates. These parameters can be obtained from field data, historical records, or, in their absence, estimated from technical literature.

2.4. Markov Chains for Failure–Repair Representation

Failure and repair dynamics can be represented using Markov chains, allowing the probabilistic evolution of the system between operational states over time to be described. In this approach, a two-state model is adopted to represent components: operation and failure, with transitions governed by failure and repair rates.

2.5. PV Module Failure–Repair Model

In the analysis of the behavior of a photovoltaic module, it is treated as a set of interconnected components, where the failure of any relevant component may reduce or even interrupt the energy supply. Photovoltaic modules are composed of bypass diodes that divide them into three sections, allowing that, if one section fails, the remaining sections can still continue generating energy. In this way, even with the failure of one diode, the module is still capable of producing energy, reducing the impact on total generation.

Each module is characterized by a failure rate. λ_{PV} and a repair rate μ_{PV}. Under the two-state Markov model (operation-failure), the probability of operation is given by Equation (1).

$$p_{PV} = \frac{\mu_{PV}}{\lambda_{PV}+\mu_{PV}} \quad (1)$$

Moreover, the probability of failure is given by Equation (2):

$$q_{PV} = \frac{\lambda_{PV}}{\lambda_{PV}+\mu_{PV}} \quad (2)$$

Where $p + q = 1$.

In addition, each module is connected through two MC4 connectors (positive and negative). Even if the cells are operating correctly, the failure of one of the connectors may interrupt energy delivery. Assuming independent behavior and identical reliability parameters for both connectors, the probability of operation of one connector is defined in Equation (3):

$$p_{MC4} = \frac{\mu_{MC4}}{\lambda_{MC4}+\mu_{MC4}} \quad (3)$$

Considering the module and its two connectors as a series configuration, the total probability of operation of the assembly is expressed in Equation (4):

$$p_{total} = p_{PV} \cdot p_{MC4}^2 \quad (4)$$

2.5.1. Bypass Diode Modeling

Consider that each photovoltaic module is divided into k electrical sections, each protected by a bypass diode. For each section i, we define:

$$q_s = 1 - p_s \;\; and \; q_d = 1 - p_d \quad (5)$$

Where p_s represents the probability that the photovoltaic section operates correctly, and p_d the probability that the corresponding bypass diode operates correctly. Section allows current conduction if it is operational itself or, in case of failure, if the associated bypass diode conducts properly. Thus, the probability that a section allows current flow is given by Equation (6):

$$p_{\text{sec}} = p_s + q_s.p_d = 1 - q_s.q_d \quad (6)$$

While the probability that the section blocks the current flow is:

$$q_{\text{sec}} = q_s . q_d. \quad (7)$$

Since the $k$sections are electrically connected in series from the current conduction perspective, the module will deliver energy to the next stage only if all sections allow current to pass. Thus, the probability that the photovoltaic module with bypass diodes operates is given by Equation (8):

$$p_{fv}^{(bp)} = \prod_{i=1}^{k} p_{sec,i}. \quad (8)$$

Assuming statistically identical sections, the expression simplifies to Equation (9):

$$p_{fv}^{(bp)} = (1-q_s . q_d)^k. \quad (9)$$

2.5.2. Integration with MC4 Connectors

Including the two MC4 connectors (positive and negative), the probability that the module–bypass diode–connector assembly delivers energy to the string is given by Equation (10):

$$p_{fvc}^{(bp)} = p_{c^-} p_{fv}^{(bp)} \cdot p_{c^+} = p_{c^-} p_{c^+} (1-q_s . q_d)^k \quad (10)$$

Complementarily, the probability of failure of the complete assembly is given by Equation (11):

$$q_{fvc}^{(bp)} = 1 - p_{fvc}^{(bp)} \quad (11)$$

2.6. String and Array Reliability Aggregation

For string reliability calculation, the reliability of modules connected in series is first considered. Subsequently, multiple strings are connected in parallel to supply the inverter. Therefore, the DC side consists of modules in series forming strings, and strings in parallel forming the array. Each module can assume two states: delivering energy to the string, with probability p_{fvc}, or not delivering energy, with probability q_{fvc}. When a module fails, it is isolated through its bypass diode. Since modules are connected in series, the string current is not interrupted; however, a voltage reduction occurs, resulting in decreased power output. The state $\beta(N_{fs})$ represents a condition in which N_{fs} modules, out of a total of N_SThey are not operating. The probability of this specific state is given by Equation (12):

$$P(\beta(N_{fs})) = p_{fvc}^{N_S - N_{fs}} . q_{fvc}^{N_{fs}}. \quad (12)$$

Because different combinations of N_{fs}failed modules may occur within the string, the probability of state $S(N_{fs})$is given by Equation (13):

$$P\left(S(N_{fs})\right) = \binom{N_S}{N_{fs}} p_{fvc}^{N_S - N_{fs}} . q_{fvc}^{N_{fs}}. \quad (13)$$

Thus, the probability that a string operates with up to $m$failed modules can be expressed by Equation (14):

$$p_{string} = \sum_{k=0}^{m} \binom{N_S}{k} q_{fvc}^{k} . p_{fvc}^{N_S - k}. \quad (14)$$

After modeling the strings, a set of $N_P$strings connected in parallel are considered. Each string is treated as a supercomponent with an operating probability. $p_{\text{string}}$and failure probability $q_{string} = 1 - p_{string}$.

The probability that the array supplies energy to the inverter (i.e., that at least one string is operating) is given by Equation (15):

$$p_{array} = 1 - \prod_{i=1}^{N_P} q_{string,i}. \quad (15)$$

Assuming statistically identical strings, the expression simplifies according to Equation (16):

$$p_{array} = 1 - (q_{string})^{N_P}. \quad (16)$$

In compact form, substituting Equation (14) into Equation (16), the array reliability can be written according to Equation (17):

$$p_{array} = 1 - \left[1 - \sum_{k=0}^{m} \binom{N_S}{k} q_{fvc}^{k} . p_{fvc}^{N_S - k}\right]^{N_P} \quad (17)$$

2.7. Inverter Reliability Model

Once the reliability of the DC array is obtained, inverter reliability is calculated. Inverters are characterized by failure rates λ_i and repair rates μ_i, from which the operating probability p_i and failure probability q_i are derived.

In this configuration, each string is connected to a single inverter; therefore, inverter failure implies the loss of the energy generated by the corresponding string. The DC switch connecting the string to the inverter is also considered, since its failure produces the same unavailability effect. Consequently, the inverter-DC switch assembly is modeled as a series configuration. The operating probability of the inverter–switch assembly is given by Equation (18):

$$p_{si} = p_i . p_{s^{dc}} \quad (18)$$

The corresponding failure probability is given by Equation (19):

$$q_{si} = 1 - p_{si}. \quad (19)$$

Considering a set of N_IInverters connected in parallel, the system continues delivering energy as long as at least one inverter is operating. Thus, the probability that the inverter stage supplies energy is given by Equation (20):

$$p_{inv} = 1 - \prod_{j=1}^{N_I} q_{si,j} \quad (20)$$

For statistically identical inverters, the expression simplifies according to Equation (21):

$$p_{inv} = 1 - (q_{si})^{N_I}. \quad (21)$$

2.8. Transformer Reliability Model

Once the reliability of the inverter assembly is obtained, the reliability of the transformers is evaluated. Transformers are responsible for stepping up the voltage level and injecting energy into the electrical grid. They are characterized by failure rates. λ_t and repair rates μ_t, from which the operating probability p_t and failure probability q_t are derived. Each transformer is supplied by a group of inverters; therefore, transformer failure results in the loss of energy from the associated inverter group. The AC-side switch or circuit breaker is also considered, since its failure produces the same unavailability effect. Consequently, the transformer-AC switch assembly is modeled as a series configuration. The operating probability of the transformer-AC switch assembly is given by Equation (22):

$$p_{st} = p_t . p_s{}^{ac}, \quad (22)$$

The failure probability is given by Equation (23):

$$q_{st} = 1 - p_{st}. \quad (23)$$

Considering N_T transformers connected in parallel, the system continues delivering energy as long as at least one transformer remains operational. Thus, the probability that the transformer stage supplies energy to the grid is given by Equation (24):

$$p_{trafo} = 1 - \prod_{k=1}^{N_T} q_{st,k}. \quad (24)$$

For statistically identical transformers, this expression simplifies according to Equation (25):

$$p_{trafo} = 1 - (q_{st})^{N_T} \quad (25)$$

2.9. Reliability Indices

2.9.1. Ideal Supplied Energy (ISE):

The ISE represents the maximum energy that the photovoltaic plant could deliver to the grid, assuming perfect operation, meaning no component failures. It only considers irradiance availability, equipment efficiency, and operating time.

$$ISE = T_o . N_S . N_I . \eta_i \sum_{k=1}^{K} (E_k . P_k . A_{fv} . \eta_k) \quad (26)$$

In Equation (26), E_k is the irradiance level from the probability distribution and P_k It is associated with probability. A_{fv} denotes the module area and η_k denotes the module efficiency at irradiance level k. N_S is the number of modules per string, N_I the number of inverters, $\eta_i$the average inverter efficiency, and T_o The total operating time is considered.

2.9.2. Expected Supplied Energy

Unlike ISE, the ESE accounts for failures in modules, inverters, and transformers. The calculation is performed in sequential stages. The energy produced by a string depends on the number of operating modules and on whether the string voltage remains above the inverter minimum voltage.

$$ESE_S = T_o \sum_{f=0}^{N_S} \Gamma(V_f)\ (N_S - f)\ P_f \quad (27)$$

In Equation (27), $f$represents the number of failed modules, P_f the probability of that failure state, and N_S The total number of modules per string. V_f is the string voltage under the considered condition, and $\Gamma(V_f)$ defines the effective power delivered by the string. The function $\Gamma(V_f)$ is defined as:

$$\Gamma(V_f) = \begin{cases} \sum_{k=1}^{K} E_k . P_k . A_{fv} . \eta_k, & \text{if } V_f \geq V_m \\ 0, & \text{otherwise} \end{cases} \quad (28)$$

In Equation (28), V_m is the minimum operating voltage of the inverter. If the string voltage drops below this threshold, no energy is delivered. After obtaining ESE_SInverter reliability is incorporated.

$$ESE_I = \sum_{g=0}^{N_I} ESE_S\ (N_I - g)\ P_g . \eta_i \quad (29)$$

In Equation (29), $g$represents the number of failed inverters, P_g the probability of that state, N_I the total number of inverters, and η_i their average efficiency. Finally, the total supplied energy is limited by the transmission capacity of the transformers.

$$ESE = \sum_{h=0}^{N_T} \min\left(ESE_I, P_{max,h}\right). (N_T - h) P_h \quad (30)$$

In Equation (30), $h$represents the number of failed transformers, P_h the probability of that condition, N_T the total number of transformers, and $P_{\max,h}$ The maximum transferable power in that state.

2.9.3. Energy Availability

Energy availability represents the fraction of the ideal energy that is effectively delivered after considering system

failures.

$$A_e = \frac{ESE}{ISE} \quad (31)$$

In Equation (31), A_e indicates the overall energy reliability of the plant, where values close to 1 represent high availability.

3. Case Study

In the present study, a 100 MWp centralized photovoltaic power plant was analyzed, comparing system availability and energy performance when using monofacial and bifacial photovoltaic modules. For the study, data from the city of Tacna, Peru, were considered due to its favorable characteristics, such as high levels of solar irradiance, low seasonal variability, and sandy soil, with predominantly clear skies and low humidity. For the analysis, irradiance data corresponding to one year were collected, as presented in Figure 4. In this figure, the irradiance is shown on an hourly basis, illustrating the variability of the solar resource over time, while the 24-hour moving average highlights the daily trend. During the analyzed period, a minimum temperature of 8.64 °C and a maximum of 24.27 °C were recorded, which are considered suitable values for the operation of photovoltaic systems. The irradiance and temperature data for the year 2023 were obtained from PVGIS (JRC–EU) [23], considering latitude −17.661°, longitude −70.337°, and an altitude of 1,583 m above sea level. For the study, a centralized topology was adopted due to its advantages in terms of scalability and cost-effectiveness, being widely used in large-scale power plants. This configuration can be observed in Figure 5.

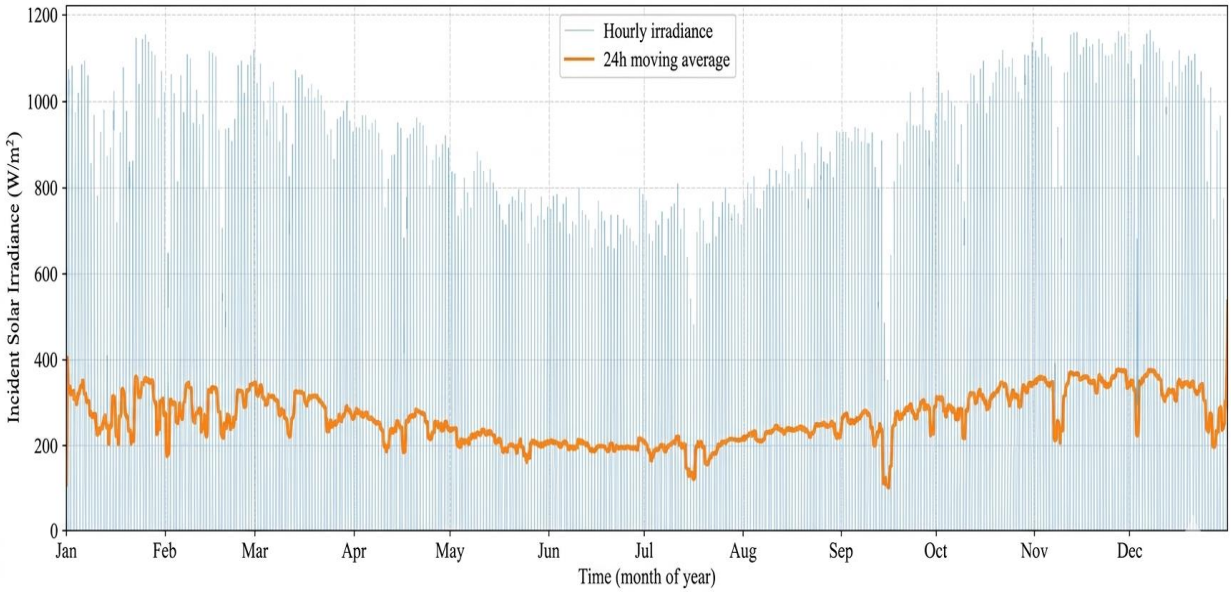

Fig. 4 Hourly solar irradiance profile and 24-hour moving average

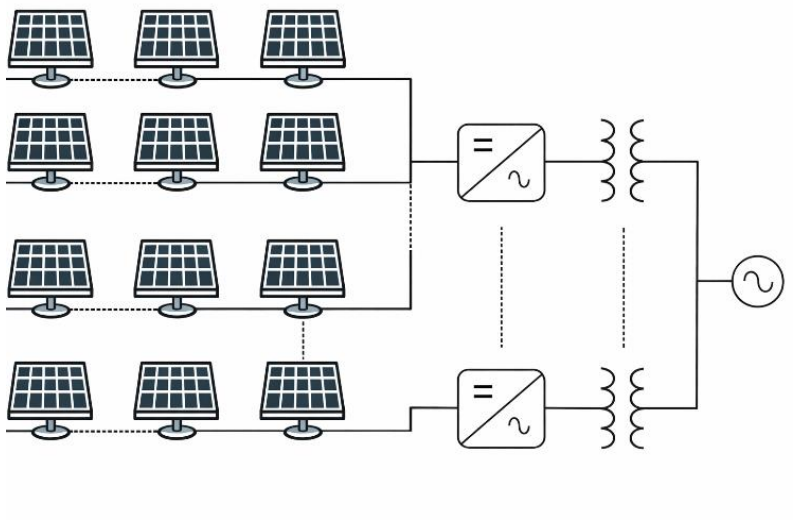

Fig. 5 Centralized topology of the analyzed photovoltaic power plant

For availability analysis, component failure and repair rates were obtained from the literature. These values are presented in Table 1. Electrical characteristics of the photovoltaic modules were also considered, including bifacial gain, which results in increased current and power output. A comparison of the electrical and dimensional parameters of monofacial and bifacial modules is presented in Table 2. A 4 MW central inverter was considered. The main electrical characteristics of the inverter, on both the DC and AC sides, are presented in Table 3.

Table 1. Failure and repair rates of PV plant components

Component	$\lambda\ [10^{-6}h^{-1}]$	$\mu\ [h^{-1}]$
PV Generator Module	26 [24]	0.0667 [24]
DC Junction Box	14.269 [25]	1.0208 [25]
Inverter	180 [24]	0.0833 [24]
DC Protection Switch	0.7 [24]	0.0208 [24]
AC Protection Switch	0.7 [24]	0.0208 [24]
Cell Protection Diode	5.4 [24]	0.1667 [24]
Transformer	0.23 [25]	285.4 [25]

Table 2. Electrical and dimensional specifications of photovoltaic modules

General Module Specifications		
Parameter	Value	Unit
Maximum Power Voltage (Vmp)	40.80	V
Open Circuit Voltage (Voc)	48.70	V
Power Temperature Coefficient	-0.29	%/°C
Module Height	2.384	m
Module Width	1.303	m
Monofacial Module	-	-
Module Efficiency	23.20	%
Maximum Power (Pmax)	720	W
Maximum Power Current (Imp)	17.67	A
Short Circuit Current (Isc)	18.69	A
Bifacial Module	-	-
Module Efficiency	27.80	
Maximum Power (Pmax)	864	
Maximum Power Current (Imp)	21.20	
Short Circuit Current (Isc)	22.43	

Table 3. Electrical specifications of the inverter-dc and ac sides

Parameter	Value	Unit
DC Side	-	-
DC Start-Up Voltage (Vdc, start)	849	V
Maximum DC Voltage (Vdc, max)	1500	V
Maximum DC Input Current (Idc, max)	4750	A
AC Side	-	-
Rated Apparent Power (cosφ = 1)	4000 / 3600	kVA
Rated Active Power (cosφ = 0.8)	3200 / 2880	kW
Rated AC Output Current (at 35°C)	3850	A
AC Output Voltage	600	V
Peak Efficiency	98.80	%

3.1. System Configuration

For solar resource modeling, hourly irradiance data over one year were used, totaling 8,760 records. These values were divided into 20 irradiance intervals, excluding periods with zero irradiance. The resulting probability mass function is shown in Figure 6. In the case of bifacial modules, a variable energy gain throughout the day was considered. A gain of 20% was adopted during sunrise and sunset periods, 10% around solar noon, and 15% during intermediate periods, representing the effect of solar angle variation and reflected radiation. To allow a direct comparison between scenarios, the same number of modules was maintained for both monofacial and bifacial cases, thereby isolating the effect of bifacial gain on performance indices. The adopted configuration uses 28

modules per string, respecting MPPT voltage limits and the maximum DC voltage of the inverter. Due to DC input current constraints, 224 strings were defined in parallel. Considering 4 MW inverters with a maximum efficiency of 98.8%, a total of 18 inverters were required to meet the installed capacity of 100 MWp.

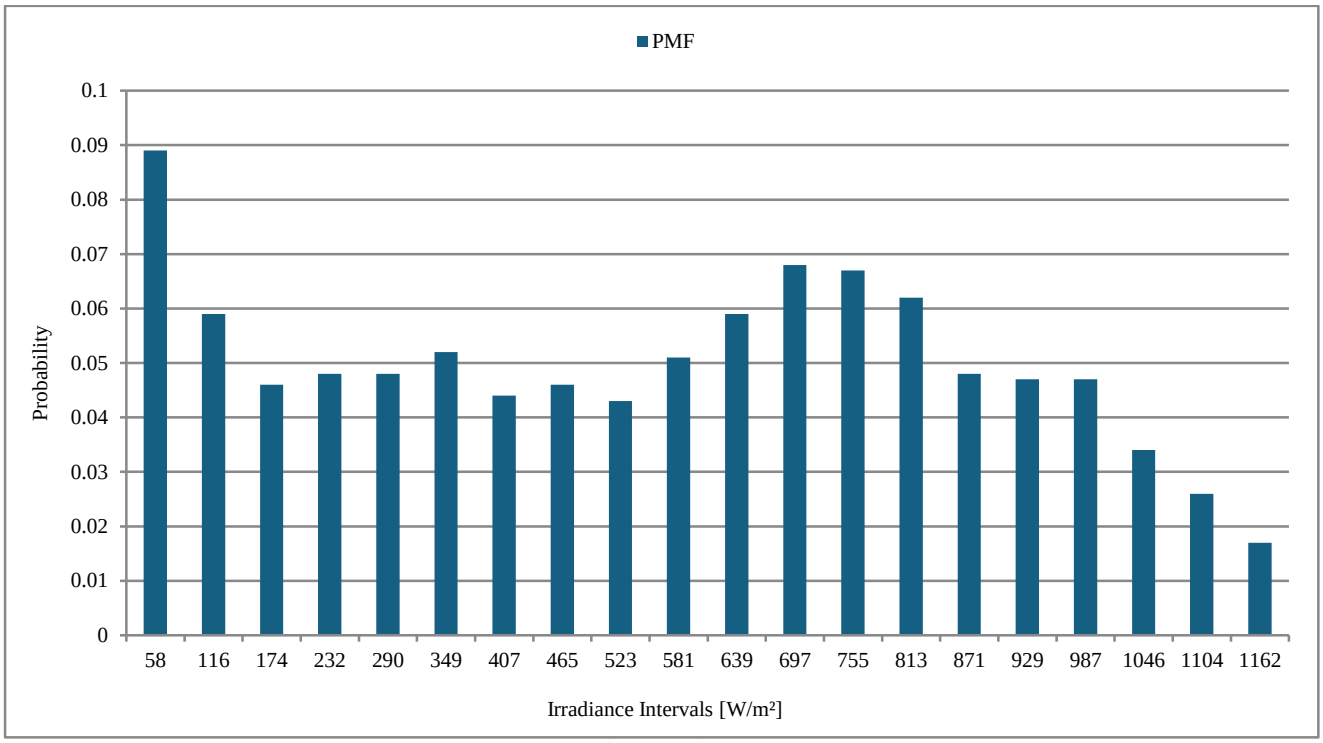

Fig. 6 Probability mass function of solar irradiance intervals

4. Results

Considering an average irradiance of 526.11 W/m², along with component failure and repair rates, the indices ISE, ESE, and Ae were obtained from the COPT. The time fraction T_0 was not considered in the intermediate stages and was included only in the final calculation.

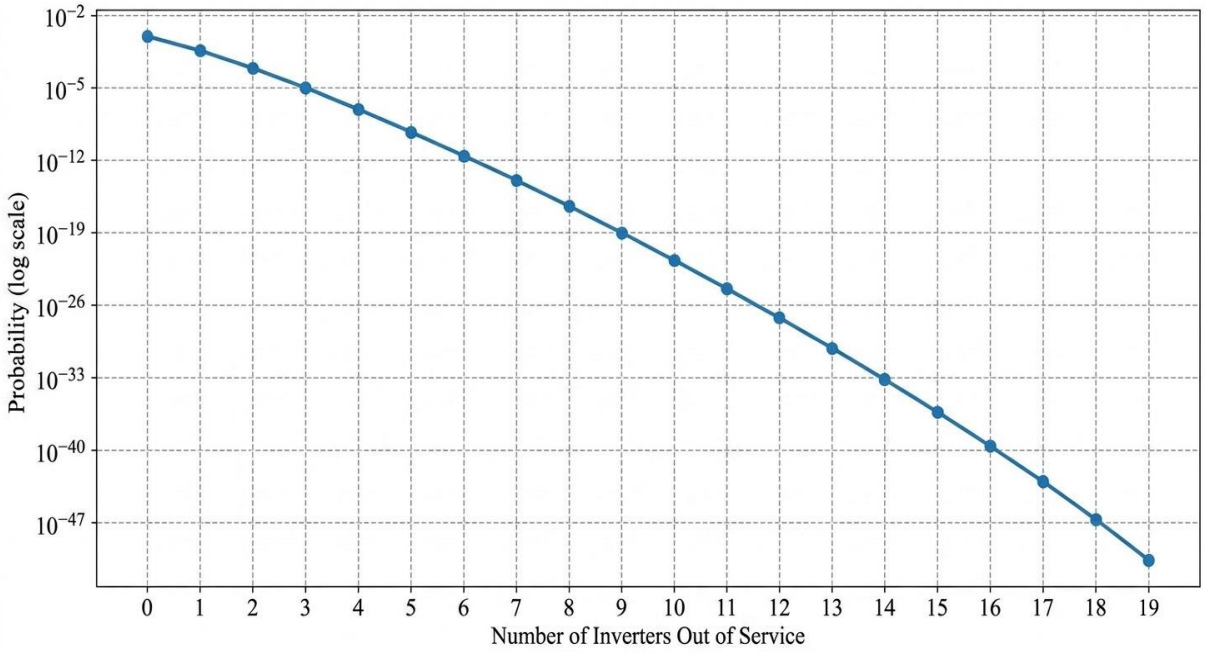

Fig. 7 State probability vs. Number of inverters out of operation

Figure 7 shows the probability as a function of the number of inverters out of operation. It can be observed that, as the number of inverters in the OFF-state increases, the probability of occurrence of these states progressively decreases. Figures 8 and 9 present the power associated with the ISE and ESE indices for monofacial and bifacial modules, respectively. In both cases, the power decreases as the number of inverters out of service increases. Nevertheless, the bifacial case maintains higher values than the monofacial case for all analyzed states. For the inverter stage, the monofacial system presented ISE = 44,641,058.05 and ESE = 44,023,905.25, while the bifacial system presented ISE = 50,575,054.85 and ESE = 49,875,865.86. These results confirm a consistent increase in the indices when bifacial gain is considered.

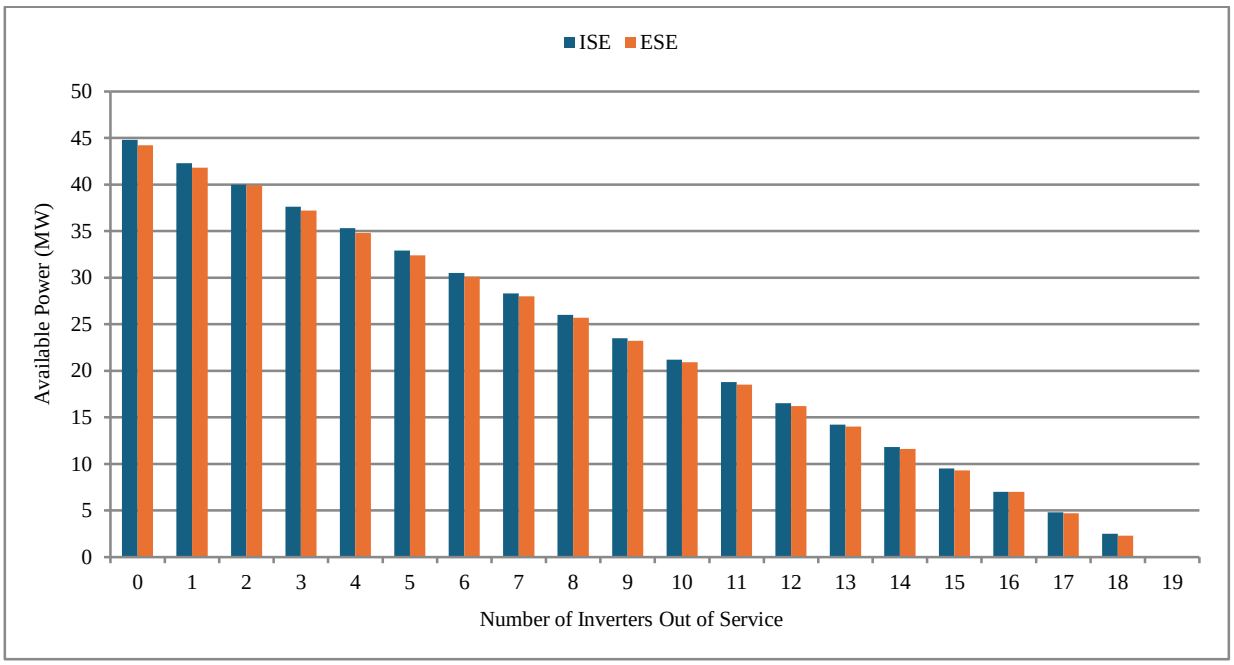

Fig. 8 ISE and ESE vs. Number of Inverters Out of Operation-Monofacial Case

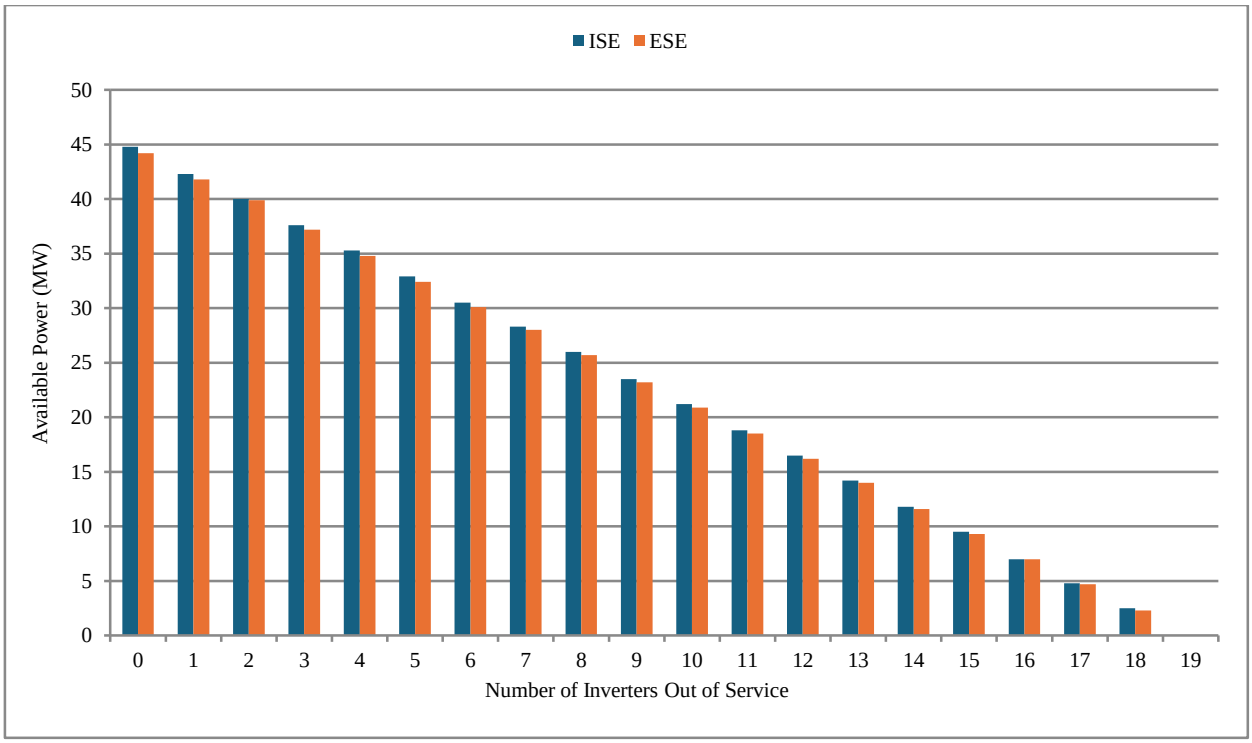

Fig. 9 ISE and ESE vs. Number of Inverters Out of Operation-Bifacial Cas

A similar behavior is observed for the transformer stage. Figure 10 presents the probability as a function of the number of transformers out of operation, while Figures 11 and 12 show the power associated with the ISE and ESE indices for the monofacial and bifacial cases. Maintaining the same number of modules and the same installed area, bifacial gain is directly reflected in increased expected and supplied energy.

The calculated energy availability was A_e= 0.9858433959 for the monofacial system and A_e= 0.9320796015 for the bifacial system. This indicates that, although the bifacial system presents higher generation potential, the final availability also depends on the failure and repair states considered in the reliability model.

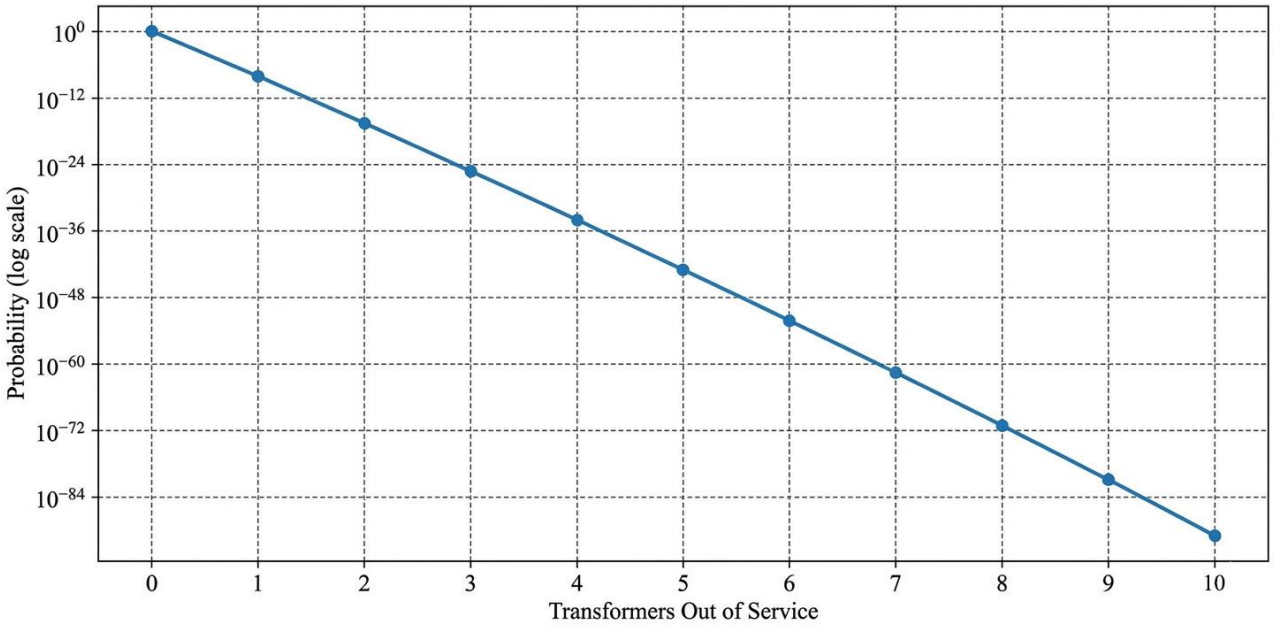

Fig. 10 State Probability vs. Number of Transformers Out of Operation

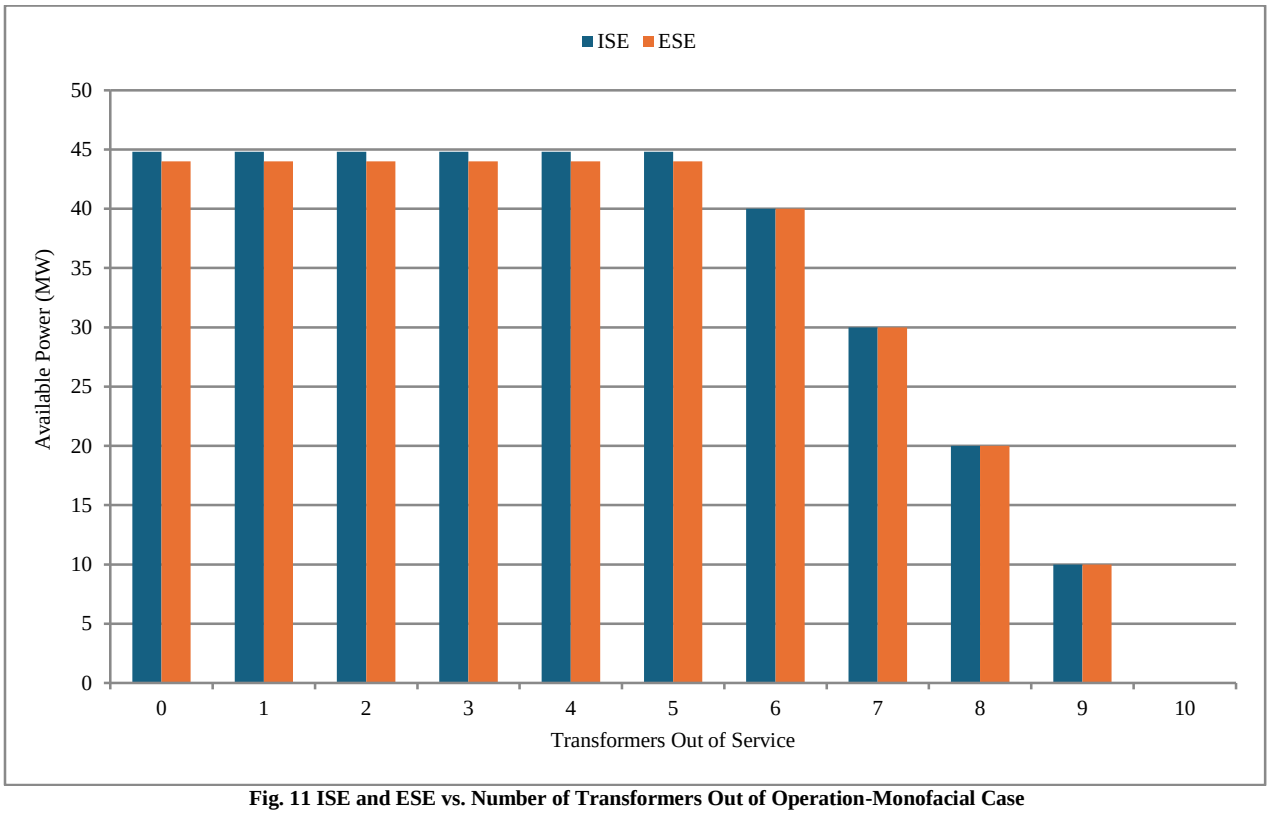

Fig. 11 ISE and ESE vs. Number of Transformers Out of Operation-Monofacial Case

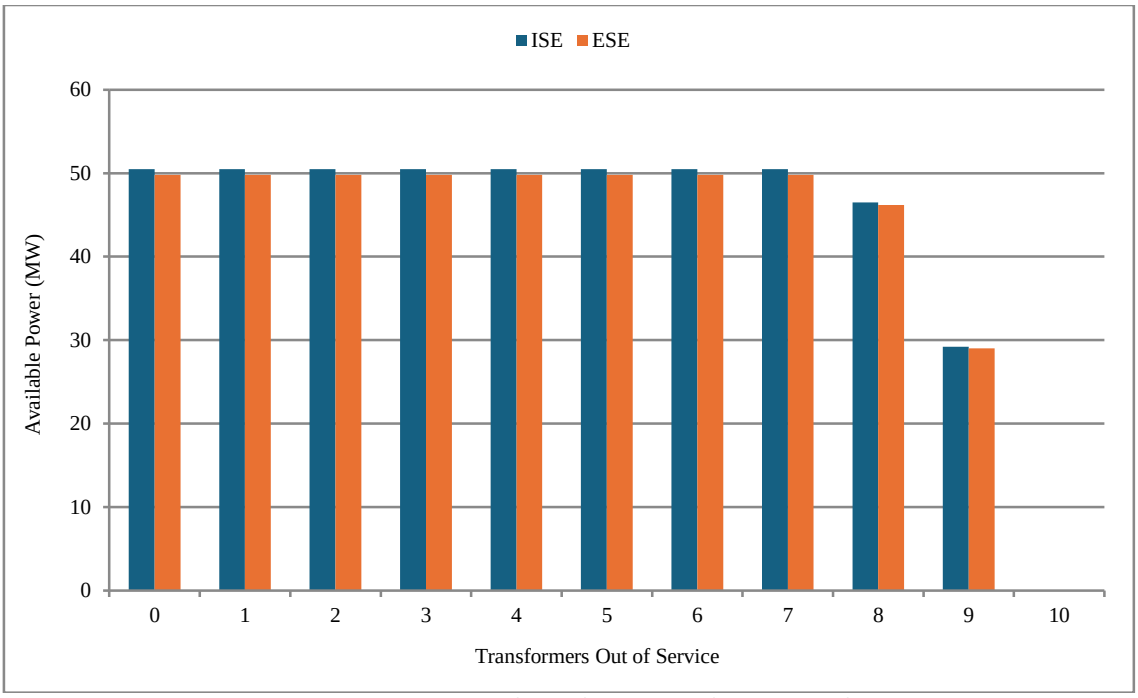

Fig. 12 ISE and ESE vs. Number of Transformers Out of Operation-Bifacial Case

5. Discussion

In the literature, the performance of monofacial and bifacial modules has been widely studied, mainly in terms of energy generation, where bifacial systems generally show better results due to the contribution of rear-side irradiance, which was also observed in this work. However, when reliability aspects are considered, the results show that higher generation does not necessarily mean better overall performance, since the bifacial system presented lower availability, possibly due to the higher level of component operation and the increased impact of failures over time. This indicates that analyzing only energy gain can lead to incomplete conclusions. In this sense, the adopted approach allows a more realistic evaluation by jointly considering energy generation and failure behavior, enabling a more consistent comparison between monofacial and bifacial systems.

6. Conclusion

Based on the results obtained, it was possible to compare bifacial and monofacial photovoltaic modules in a 100 MWp power plant located in Tacna. The analysis shows that bifacial modules provide a clear increase in energy indices, with ISE rising from 44,641,058.05 to 50,575,054.85 and ESE from 44,023,905.25 to 49,875,865.86, corresponding to an increase of about 13.3%. This confirms the advantage of bifacial technology in terms of energy generation. However, when energy availability is considered, the monofacial system presents a higher value (Ae = 0.9858) compared to the bifacial system (Ae = 0.9321), even under the same failure and repair conditions. This indicates that higher energy production does not necessarily result in higher effective availability, since system performance is also influenced by the probabilistic behavior of component failures and repairs.

Therefore, the evaluation of bifacial systems should not be based only on energy gain, but also on reliability aspects. Even so, both configurations present high availability levels, and the bifacial system maintains superior energy performance overall. In this sense, combining reliability modeling with energy performance analysis provides a more complete and realistic assessment of photovoltaic power plants, especially in large-scale applications where it is necessary not only to maximize generation, but also to ensure consistent energy delivery over time.

Acknowledgment

The authors gratefully acknowledge the Universidad Nacional de San Agustín de Arequipa (UNSA) for support and collaboration throughout this research.

References

[1] Saeed Al-Ali, Abdul Ghani Olabi, and Montaser Mahmoud, "A Review of Solar Photovoltaic Technologies: Developments, Challenges, and Future Perspectives," *Energy Conversion and Management: X*, vol. 27, pp. 1-16, 2025. [CrossRef] [Google Scholar] [Publisher Link]

[2] IEA Photovoltaic Power Systems Programme (IEA PVPS), Snapshot of Global PV Markets 2025, Task 1 Strategic PV Analysis and Outreach, 2025. [Online]. Available: https://iea-pvps.org/wp-content/uploads/2025/04/Snapshot-of-Global-PV-Markets_2025.pdf

[3] Ayman Mdallal et al., "A Comprehensive Review on Solar Photovoltaics: Navigating Generational Shifts, Innovations, and Sustainability," *Sustainable Horizons*, vol. 13, pp. 1-20, 2025. [CrossRef] [Google Scholar] [Publisher Link]

[4] Aydan Garrod, and Aritra Ghosh, "A Review of Bifacial Solar Photovoltaic Applications," *Frontiers in Energy*, vol. 17, no. 6, pp. 704-726, 2023. [CrossRef] [Google Scholar] [Publisher Link]

[5] Sukanta Roy et al., "Photovoltaic Inverter Failure Mechanism Estimation Using Unsupervised Machine Learning and Reliability Assessment," *IEEE Transactions on Reliability*, vol. 73, no. 3, pp. 1418-1432, 2024. [CrossRef] [Google Scholar] [Publisher Link]

[6] Michelle Kitayama da Silva, Mehreen Saleem Gul, and Hassam Chaudhry, "Review on the Sources of Power Loss in Monofacial and Bifacial Photovoltaic Technologies," *Energies*, vol. 14, no. 23, pp. 1-29, 2021. [CrossRef] [Google Scholar] [Publisher Link]

[7] M. Kivambe, A. Abdallah, B. Figgis, G. Scabbia, M. Abdelrahim, and J. Lopez-Garcia, "Assessing Vertical East-West Bifacial Photovoltaic Systems in Desert Environments: Energy Yield and Soiling Mitigation," *Solar Energy*, vol. 279, pp. 1-10, 2024. [CrossRef] [Google Scholar] [Publisher Link]

[8] Abdelrahman O. Ali et al., "Advancements in Photovoltaic Technology: A Comprehensive Review of Recent Advances and Future Prospects," *Energy Conversion and Management: X*, vol. 26, pp. 1-28, 2025. [CrossRef] [Google Scholar] [Publisher Link]

[9] Douglas Lamas Dias et al., "Performance Assessment of Bifacial and Monofacial PV Systems on Different Types of Soils in a Low-Latitude Site," *Renewable Energy*, vol. 246, 2025. [CrossRef] [Google Scholar] [Publisher Link]

[10] Rahimat O. Yakubu et al., "A Systematic Literature Review of the Bifacial Photovoltaic Module and its Applications," *The Journal of Engineering*, vol. 2024, no. 8, pp. 1-20, 2024. [CrossRef] [Google Scholar] [Publisher Link]

[11] Ghadeer Badran, and Mahmoud Dhimish, "A Comparative Study of Bifacial Versus Monofacial PV Systems at the UK's Largest Solar Plant," *Clean Energy*, vol. 8, no. 4, pp. 248-260, 2024. [CrossRef] [Google Scholar] [Publisher Link]

[12] Dariusz Kurz et al., "An Analysis of the Increase in Energy Efficiency of Photovoltaic Installations by Using Bifacial Modules," *Energies*, vol. 18, no. 5, pp. 1-25, 2025. [CrossRef] [Google Scholar] [Publisher Link]

[13] Muneeshwar Ramavath, and Rama Krishna Puvvula Venkata, "Comparative Reliability and Performance Analysis of PV Inverters with Bifacial and Monofacial Panels," *International Journal of Power Electronics and Drive Systems*, vol. 16, no. 3, pp. 1970-1982, 2025. [CrossRef] [Google Scholar] [Publisher Link]

[14] Alejandro González-Moreno et al., "Outdoor Performance Comparison of Bifacial and Monofacial Photovoltaic Modules in Temperate Climate and Industrial-Like Rooftops," *Applied Sciences*, vol. 14, no. 13, pp. 1-16, 2024. [CrossRef] [Google Scholar] [Publisher Link]

[15] Pramod R. Sonawane et al., "Reliability and Criticality Analysis of a Large-Scale Solar Photovoltaic System Using Fault Tree Analysis Approach," *Sustainability*, vol. 15, no. 5, pp. 1-24, 2023. [CrossRef] [Google Scholar] [Publisher Link]

[16] Amir A. Abdallah et al., "Performance of Monofacial and Bifacial Silicon Heterojunction Modules Under Desert Conditions and the Impact of PV Soiling," *Sustainability*, vol. 15, no. 10, pp. 1-13, 2023. [CrossRef] [Google Scholar] [Publisher Link]

[17] Dharani Kolantla et al., "Critical Review on Various Inverter Topologies for PV System Architectures," *IET Renewable Power Generation*, vol. 14, no. 17, pp. 3418-3438, 2021. [CrossRef] [Google Scholar] [Publisher Link]

[18] L. Hassaine et al., "Overview of Power Inverter Topologies and Control Structures for Grid Connected Photovoltaic Systems," *Renewable and Sustainable Energy Reviews*, vol. 30, pp. 796-807, 2013. [CrossRef] [Google Scholar] [Publisher Link]

[19] Marzia Alam, Mehreen Saleem Gul, and Tariq Muneer, "Performance Analysis and Comparison Between Bifacial and Monofacial Solar Photovoltaic at Various Ground Albedo Conditions," *Renewable Energy Focus*, vol. 44, pp. 295-316, 2023. [CrossRef] [Google Scholar] [Publisher Link]

[20] Dominik Keiner et al., "Assessing the Impact of Bifacial Solar Photovoltaics on Future Power Systems Based on Capacity-Density-Optimised Power Plant Yield Modelling," *Solar Energy*, vol. 295, pp. 1-35, 2025. [CrossRef] [Google Scholar] [Publisher Link]

[21] Anupam Yedida, and Revathy Padmanabhan, "Performance Limits in Bifacial Tandem Solar Cell Modules for Multiple Configurations," *IEEE Journal of Photovoltaics*, vol. 16, no. 1, pp. 98-112, 2026. [CrossRef] [Google Scholar] [Publisher Link]

[22] Alessandro Birolini, *Reliability Engineering: Theory and Practice*, Springer, 2017. [CrossRef] [Google Scholar] [Publisher Link]

[23] European Commission, PVGIS-Photovoltaic Geographical Information System, Joint Research Centre (JRC), 2025. [Online]. Available: https://re.jrc.ec.europa.eu/pvg_tools/en/#MR

[24] A. Sayed et al., "Reliability, Availability and Maintainability Analysis for Grid-Connected Solar Photovoltaic Systems," *Energies*, vol. 12, no. 7, pp. 1-18, 2019. [CrossRef] [Google Scholar] [Publisher Link]

[25] Simona-Vasilica Oprea et al., "Photovoltaic Power Plants (PV-PP) Reliability Indicators for Improving Operation and Maintenance Activities: A Case Study of PV-PP Agigea Located in Romania," *IEEE Access*, vol. 7, pp. 39142-39156, 2019. [CrossRef] [Google Scholar] [Publisher Link]